

6-12-2003

# Synthesis and Characterization of the Thiogermanic Acids $H_4Ge_4S_{10}$ and $H_2Ge_4S_9$

Steven A. Poling  
*Iowa State University*

Carly R. Nelson  
*Iowa State University*

Jacob T. Sutherland  
*Iowa State University*

Steve W. Martin  
*Iowa State University*, [swmartin@iastate.edu](mailto:swmartin@iastate.edu)

Follow this and additional works at: [http://lib.dr.iastate.edu/mse\\_pubs](http://lib.dr.iastate.edu/mse_pubs)

 Part of the [Materials Science and Engineering Commons](#), and the [Physical Chemistry Commons](#)

The complete bibliographic information for this item can be found at [http://lib.dr.iastate.edu/mse\\_pubs/73](http://lib.dr.iastate.edu/mse_pubs/73). For information on how to cite this item, please visit <http://lib.dr.iastate.edu/howtocite.html>.

---

This Article is brought to you for free and open access by the Materials Science and Engineering at Iowa State University Digital Repository. It has been accepted for inclusion in Materials Science and Engineering Publications by an authorized administrator of Iowa State University Digital Repository. For more information, please contact [digirep@iastate.edu](mailto:digirep@iastate.edu).

---

# Synthesis and Characterization of the Thiogermanic Acids $\text{H}_4\text{Ge}_4\text{S}_{10}$ and $\text{H}_2\text{Ge}_4\text{S}_9$

## Abstract

The synthesis and structure of the thiogermanic acids  $\text{H}_4\text{Ge}_4\text{S}_{10}$  and  $\text{H}_2\text{Ge}_4\text{S}_9$  are reported. A novel preparation method consisting of reacting germanium oxide with liquid hydrogen sulfide containing a trace amount of water is used to form  $\text{Ge}_4\text{S}_{10}^{4-}$  ions. Evaporating the hydrogen sulfide solution at room temperature leaves an unstable  $\text{H}_4\text{Ge}_4\text{S}_{10} \cdot x\text{H}_2\text{O}$  product. The stoichiometry and structure of the thermally stable anhydrous phase are dependent on reaction time. An  $\text{H}_4\text{Ge}_4\text{S}_{10}$  product with an adamantane-like cage structure is obtained at shorter reaction times. Longer reaction times produce an  $\text{H}_2\text{Ge}_4\text{S}_9$  product with a more complex cage unit, a higher symmetry unit cell, and increased thermal stability. Raman, infrared, powder X-ray diffraction, and thermogravimetric data are reported for both structures.

## Disciplines

Materials Science and Engineering | Physical Chemistry

## Comments

Reprinted with permission from *Journal of Physical Chemistry B* 107 (2003): 5413–5418, doi:[10.1021/jp027313w](https://doi.org/10.1021/jp027313w). Copyright 2003 American Chemical Society.

# Synthesis and Characterization of the Thiogermanic Acids $\text{H}_4\text{Ge}_4\text{S}_{10}$ and $\text{H}_2\text{Ge}_4\text{S}_9$

Steven A. Poling, Carly R. Nelson, Jacob T. Sutherland, and Steve W. Martin\*

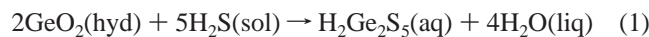
Department of Materials Science and Engineering, Iowa State University, Ames, Iowa 50011

Received: October 25, 2002; In Final Form: December 23, 2002

The synthesis and structure of the thiogermanic acids  $\text{H}_4\text{Ge}_4\text{S}_{10}$  and  $\text{H}_2\text{Ge}_4\text{S}_9$  are reported. A novel preparation method consisting of reacting germanium oxide with liquid hydrogen sulfide containing a trace amount of water is used to form  $\text{Ge}_4\text{S}_{10}^{4-}$  ions. Evaporating the hydrogen sulfide solution at room temperature leaves an unstable  $\text{H}_4\text{Ge}_4\text{S}_{10} \cdot x\text{H}_2\text{O}$  product. The stoichiometry and structure of the thermally stable anhydrous phase are dependent on reaction time. An  $\text{H}_4\text{Ge}_4\text{S}_{10}$  product with an adamantane-like cage structure is obtained at shorter reaction times. Longer reaction times produce an  $\text{H}_2\text{Ge}_4\text{S}_9$  product with a more complex cage unit, a higher symmetry unit cell, and increased thermal stability. Raman, infrared, powder X-ray diffraction, and thermogravimetric data are reported for both structures.

## 1. Introduction

Current and past efforts to produce protonated germanium sulfide complexes using hydrogen sulfide have resulted in the stoichiometric compound  $\text{H}_4\text{Ge}_4\text{S}_{10}$ . The existence of a  $\text{Ge}_4\text{S}_{10}^{4-}$  unit cage was first reported as a  $\text{Ge}_2\text{S}_5^{2-}$  ion in solution.<sup>1</sup> The reported  $\text{H}_2\text{Ge}_2\text{S}_5$  thio-acid was synthesized by reacting a hydrous form of  $\text{GeO}_2$  in an ethyl alcohol solution saturated with  $\text{H}_2\text{S}$ . The reaction was written as



Structural data were not reported for the reaction product  $\text{H}_2\text{Ge}_2\text{S}_5$ , it was simply noted to be a white amorphous solid. It was also reported to decompose slowly at 0 °C and was extremely soluble in water. This synthesis route proved to be inadequate for obtaining very pure samples without oxide contamination.

In the present study, a reaction medium consisting of liquid  $\text{H}_2\text{S}$  with a trace amount of water is implemented at room temperature. Under these conditions, it is possible to produce  $\text{Ge}_4\text{S}_{10}^{4-}$  ions starting from quartz-type  $\text{GeO}_2$  or glassy  $\text{GeS}_2$ . This new preparation method is simple and functional, producing a structural evolution of the  $\text{Ge}_4\text{S}_{10}^{4-}$  cage unit over time. In this article, the stoichiometry and structure of the resulting thiogermanic acid starting from  $\text{GeO}_2$  as a precursor are characterized as functions of the reaction time.

There have been two reported structural isomers for the  $\text{Ge}_4\text{S}_{10}^{4-}$  complex: adamantane and “double-decker.” Figure 1 shows the structures of the adamantane and double-decker  $\text{Ge}_4\text{S}_{10}^{4-}$  complex anions. An adamantane-like unit was recently determined for the  $\text{H}_4\text{Ge}_4\text{S}_{10}$  phase.<sup>2</sup> Adamantane units have also been determined for the phases of  $\text{M}_4\text{Ge}_4\text{S}_{10}$  ( $\text{M} = \text{Na}, \text{K}, \text{Rb}, \text{Cs}, \text{and Tl}$ )<sup>3–6</sup> and  $\text{Ba}_2\text{Ge}_4\text{S}_{10}$ .<sup>7</sup> The adamantane unit is composed of four corner-shared  $\text{GeS}_4^{4-}$  tetrahedra. This structural unit was reported to be synthesized from solid-state reactions in evacuated silica tubes. Aqueous solution reactions were also reported for  $\text{Cs}_4\text{Ge}_4\text{S}_{10} \cdot 3\text{H}_2\text{O}$ , which was synthesized by adding  $\text{GeS}_2$  to a concentrated aqueous solution of  $\text{Cs}_2\text{S}$

where upon crystallization of the adduct was observed on standing.<sup>8</sup> These units are usually highly symmetric with point symmetry group of  $T_d$ .<sup>9</sup> Hence, the vibrational modes of the adamantane  $\text{Ge}_4\text{S}_{10}^{4-}$  unit are distributed among the following Raman (R) and infrared (IR) fundamental vibrations:  $\Gamma(T_d) = 3A_1(\text{R}) + 3E(\text{R}) + 3F_1(\text{inactive}) + 6F_2(\text{IR}, \text{R})$ . A triclinic unit cell with space group  $P\bar{1}$  is observed for the adamantane  $\text{H}_4\text{Ge}_4\text{S}_{10}$  phase.<sup>2</sup> Orthorhombic and monoclinic crystal systems with space groups  $Cmcm$ ,  $C2/c$ , and  $C12/c1$  have been revealed for the  $\text{M}_4\text{Ge}_4\text{S}_{10}$  adamantane compounds.<sup>4–6,10</sup> A cubic unit cell with space group  $Fd\bar{3}$  or  $Fd\bar{3}m$  has been reported for  $\text{Ba}_2\text{Ge}_4\text{S}_{10}$ .<sup>7</sup>

Although germanium oxide-based complexes are known to form higher homologous structures, the only additional reported structure for  $\text{Ge}_4\text{S}_{10}^{4-}$  based complexes is the double-decker.<sup>11</sup> This isomer has been previously reported for organo-substituted germanium sesquisulfides,  $\text{R}_4\text{Ge}_4\text{S}_6$ , where R represents an organic group.<sup>11,12</sup> From a ring-strain perspective, the double-decker isomer is less favorable, having two sets of edge-shared tetrahedral units linked together. Structural solutions from X-ray diffraction (XRD) of  $\text{R}_4\text{Ge}_4\text{S}_6$  indicate S–S distances in the shared edges of 3.30 Å,<sup>12</sup> which is less than the sum of the van der Waals radii of 3.60 Å. Additionally, <sup>77</sup>Se NMR distinguishes two distinct selenium environments for  $\text{R}_4\text{Ge}_4\text{Se}_6$  and  $\text{R}_4\text{Si}_4\text{Se}_6$  double-decker complexes.<sup>12</sup> The double-decker  $\text{Ge}_4\text{S}_{10}^{4-}$  unit has a point symmetry group of  $D_{2h}$ <sup>11</sup> and the vibrational modes are distributed among the following fundamental vibrations:  $\Gamma(D_{2h}) = 7A_g(\text{R}) + 3A_u(\text{inactive}) + 5B_{1g}(\text{R}) + 4B_{1u}(\text{IR}) + 3B_{2g}(\text{R}) + 5B_{2u}(\text{IR}) + 3B_{3g}(\text{R}) + 6B_{3u}(\text{IR})$ . Cubic and monoclinic crystal systems with space groups  $I23$  and  $C2/c$ , respectively, have been revealed for the organo-substituted  $\text{R}_4\text{Ge}_4\text{S}_6$  double-decker compounds.<sup>11,12</sup>

## 2. Experimental Section

**2.1. Sample Preparation.** A typical reaction consisted of placing 500 mg ( $\pm 1$  mg) of commercial quartz-type  $\text{GeO}_2$  powder (Cerac 99.999%,  $\sim 325$  mesh) in an alumina tube, which in turn was placed inside a type 316 stainless steel reaction vessel. The total free volume inside the reaction vessel was  $\sim 72$  mL. The reactor was sealed with a Teflon O-ring gasket and a Swagelok type 316 stainless steel needle valve. The assembled

\* Corresponding author. E-mail: swmartin@iastate.edu. Phone: (515) 294–0745.

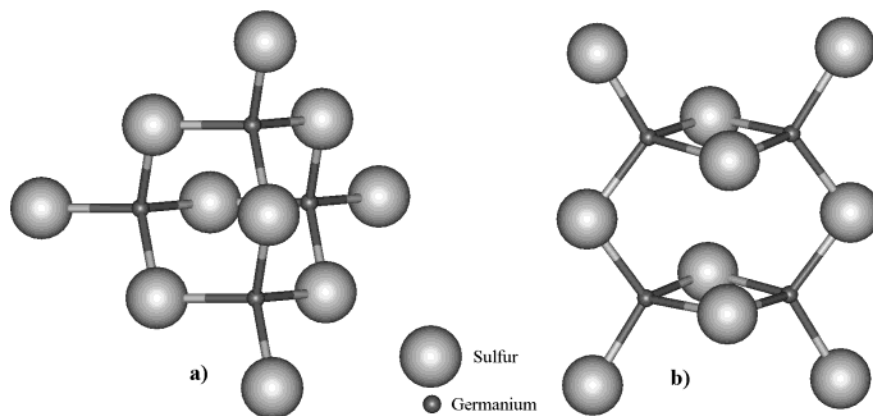


**Figure 1.** (a) Ball-and-stick schematic of an adamantane  $\text{Ge}_4\text{S}_{10}^{4-}$  structural unit. Cations of H, Na, K, Rb, Cs, Tl, and Ba have been shown to form these units with  $\text{GeS}_2$ . (b) Ball-and-stick schematic of a double-decker  $\text{Ge}_4\text{S}_{10}^{4-}$  structural unit. Organo-substituted  $\text{GeS}_2$  compounds have been shown to form these units.

reactor was evacuated to  $\sim 75$  mTorr, cooled with liquid nitrogen ( $T < -86$  °C), and back-filled with  $\sim 7$  g of  $\text{H}_2\text{S}$  gas (Matheson, 99.9 mol %). For these experiments, the reaction rate was dependent on the impurity water content found in the commercial purity  $\text{H}_2\text{S}$  gas cylinder ( $\sim 0.02$  mol %). The reactions took place at room temperature ( $\sim 22$  °C) where liquid  $\text{H}_2\text{S}$  was present in the reactor under its own vapor pressure ( $\sim 267$  psia). The total reaction time was varied from 1 to 8 weeks. Reaction times may be decreased by the further addition of a small amount of water (e.g.  $\sim 1$  mol % of  $\text{H}_2\text{O}$  to  $\text{H}_2\text{S}$ ) to the impurity water content of the  $\text{H}_2\text{S}$ . After the designated reaction time, the resulting  $\text{H}_2\text{S}$ – $\text{H}_2\text{O}$  solution inside the reactor was evaporated through a  $\text{NH}_4\text{OH}$  solution. The reactor was then opened inside a glovebox with low oxygen and water content ( $< 5$  ppm), where mass measurements of the resulting product were recorded as a function of time. Intercalated  $\text{H}_2\text{O}$  may take up to a day to fully dissipate; heating may be used to speed this process.

**2.2. Spectroscopic Measurements.** Structural investigations were conducted using Raman scattering, infrared absorption, and powder XRD. Raman spectra were obtained using a Bruker FT-Raman RFS 100/S spectrometer with a 1064-nm Nd:YAG laser using  $2\text{ cm}^{-1}$  resolution and 300 mW of power focused on  $\sim 0.1$  mm diameter spot size. Powdered samples were packed into an aluminum sample holder and covered with amorphous tape. Infrared absorption spectra were obtained using a Bio-Rad FTS-40 mid-infrared (mid-IR) spectrometer and a Bio-Rad FTS-60V far-infrared (far-IR) spectrometer using  $4\text{ cm}^{-1}$  resolution. Pressed KBr powder pellets were prepared using  $\sim 3$  wt % of sample for mid-IR, and powder mixed with Nujol sandwiched between two high-density polyethylene sheets was used for the far-IR. Powder XRD spectra were collected from  $3^\circ$  to  $70^\circ$   $2\theta$  using a Siemens D500 diffractometer with Cu  $K\alpha$  radiation ( $\lambda = 1.54178$  Å). Powdered samples were packed into a polycarbonate sample disk with no amorphous cover. Care was taken to minimize atmospheric exposure; after 1 h scan time no structural changes were observed.

**2.3. Thermal Measurements.** Thermal investigations were performed using a Perkin-Elmer Thermogravimetric Analyzer TGA 7 (TGA). A 20 mL/min flow of  $\text{N}_2$  was used as the sample purge to prevent any oxidation reactions. About 25 mg of each sample was placed inside an aluminum sample pan. A heating rate of  $10$  °C/min was used for all TGA experiments.

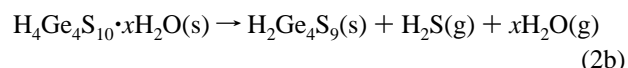
### 3. Results and Discussion

**3.1. Mass Change.** Sample masses were recorded for all reactions as a function of reaction time. There was minimal

reaction for the first week at room temperature: e.g.,  $\sim 2$  wt % increase. This mass increase was most likely due to hydroxyl group formation in the  $\text{GeO}_2$  as can be seen in the mid-IR spectra in Figure 3; the initial  $\text{H}_2\text{O}$  contamination was accredited to the commercial purity  $\text{H}_2\text{S}$  gas. Hydroxyl group formation is also in agreement with the observation that hydrated  $\text{GeO}_2$  was necessary for the reaction to proceed.<sup>1</sup> A white-to-beige colored product was collected for reaction times longer than 1 week. Two-week reactions produced stabilized sample masses consistent with  $\sim 92$  wt %  $\text{H}_4\text{Ge}_4\text{S}_{10}$  with the balance as  $\text{GeO}_2$ ; this is in agreement with the mid-IR spectra in Figure 3. Stabilized masses from 3- and 4-week reaction times suggest mixed-phase products, whereas 8-week reactions indicated an  $\text{H}_2\text{Ge}_4\text{S}_9$  phase. As an example, a complete conversion to the stoichiometric compound  $\text{H}_2\text{Ge}_4\text{S}_9$  from  $500 \pm 1$  mg of  $\text{GeO}_2$  would yield  $694 \pm 2$  mg of product. A mixed oxy-sulfide phase of  $\text{H}_4\text{Ge}_4\text{S}_8\text{O}_2$  would yield a similar mass, but no evidence for this type of phase is present in the corresponding vibrational spectra. Immediately after opening the reactors, the recorded sample masses were much higher. This is consistent with hydrous  $\text{H}_4\text{Ge}_4\text{S}_{10} \cdot x\text{H}_2\text{O}$  phases stabilized by the cooler temperature resulting from endothermic boiling-off of  $\text{H}_2\text{S}$  during rapid removal. For the 2- and 8-week reaction products, the decomposition reaction upon warming to room temperature may be written as



and



respectively. About 1 day after removing the liquid  $\text{H}_2\text{S}$ , all intercalated  $\text{H}_2\text{O}$  was evaporated and the decomposition reaction was complete.

**3.2. Raman Scattering.** Figure 2 presents the unpolarized Raman spectra of the stabilized products as a function of reaction time in liquid  $\text{H}_2\text{S}$  at room temperature. The vibrational frequencies in the spectra are time independent after opening the reactor; for reaction times greater than one week, this implies the  $\text{Ge}_4\text{S}_{10}^{4-}$  structural cage unit is present in both the hydrous and anhydrous phases. For 1 week of reaction time, the vibrational bands assigned to quartz-type  $\text{GeO}_2$  are still present and the strongest band located at  $\sim 443\text{ cm}^{-1}$  can be assigned to Ge–O–Ge symmetric stretching.<sup>13</sup> For 2 weeks of reaction time, new vibrational bands appear, suggesting a structure that is consistent with adamantane-like  $\text{Ge}_4\text{S}_{10}^{4-}$  units. Table 1

TABLE 1: Raman and IR Mode Assignments for the 2-Week Reaction Product  $\text{H}_4\text{Ge}_4\text{S}_{10}$ <sup>a</sup>

	$\text{H}_4\text{Ge}_4\text{S}_{10}$ and $\text{H}_4\text{Ge}_4\text{S}_{10} \cdot x\text{H}_2\text{O}$ adamantane		$\text{Cs}_4\text{Ge}_4\text{S}_{10}$ adamantane <sup>9</sup>		$\text{Na}_4\text{Ge}_4\text{S}_{10}$ adamantane <sup>3</sup>	lithium dithiogermante glass <sup>21</sup>	silver dithiogermanate glass <sup>18</sup>	
	Raman	IR	Raman	IR	Raman	Raman	Raman	IR
$\nu_{15}(\text{F}_2)$	107		116	121				
$\nu_{14}(\text{F}_2)$	145		144	148				
$\nu_3(\text{A}_1)$	187		193		200			
$\nu_2(\text{A}_1) \{ \nu_s(\text{Ge-S-Ge}) \}$	355		340		354	350	339	330
$\nu_1(\text{A}_1) \{ \nu_s(\text{Ge-S}^-) \}$	407, 416	414	462		470	425	415	412
$\nu(\text{S-H})$	2484, 2515	2479, 2511						

<sup>a</sup>  $T_d$  point group symmetry is assumed for the adamantane  $\text{Ge}_4\text{S}_{10}^{4-}$  unit cage. Assignments for comparable reference systems are also presented. All units are in wavenumbers ( $\text{cm}^{-1}$ ).

TABLE 2: Raman and IR Mode Assignments for the 8-Week Reaction Product  $\text{H}_2\text{Ge}_4\text{S}_9$ <sup>a</sup>

	$\text{H}_2\text{Ge}_4\text{S}_9$ and $\text{H}_4\text{Ge}_4\text{S}_{10} \cdot x\text{H}_2\text{O}$		Glassy $\text{GeS}_2$		High Temp 2D phase ( $\beta\text{-GeS}_2$ )		Low Temp 3D phase ( $\alpha\text{-GeS}_2$ )	
	Raman	IR	Raman	IR	Raman	IR	Raman	IR
bond-bending	106, 127, 152,		105 <sup>19</sup> , 112 <sup>16</sup> ,	149 <sup>19</sup> , 147 <sup>16</sup> ,				
E and low $\text{F}_2$	172, 197, 240		110, 150 <sup>18</sup>	115, 153 <sup>18</sup>				
$\text{A}_1$ corner-shared { $\nu_s(\text{Ge-S-Ge})$ }	344	338	342 <sup>18,14,19</sup> ,	328 <sup>19</sup> ,	356 <sup>15</sup> , 361 <sup>20</sup> ,	342 <sup>20</sup>	339 <sup>15</sup> ,	332 <sup>20</sup>
$\text{A}_1$ edge-shared { $\nu_s(\text{Ge-S-Ge})$ }	352		343 <sup>16</sup> ,	340 <sup>18,16</sup> ,	363 <sup>22</sup> ,		342 <sup>20</sup>	
$\text{F}_2$ { $\nu_{as}(\text{Ge-S-Ge})$ }	363	370	374 <sup>b,14</sup> ,	372 <sup>16</sup>	363 <sup>15</sup> ,			
bond-stretching	380	386	370 <sup>b,16</sup>	367 <sup>19</sup> , 395 <sup>16</sup> ,	383 <sup>22</sup>			
$\text{A}_1$ and high $\text{F}_2$	401	403	375 <sup>19</sup> , 390 <sup>16</sup> ,	367 <sup>19</sup> , 395 <sup>16</sup> ,	340-450,	350-450 <sup>20</sup>	340-450,	350-450 <sup>20</sup>
	409	411	368 <sup>18</sup>	377 <sup>18</sup>	exc. $\text{A}_1$ <sup>20</sup>		exc. $\text{A}_1$ <sup>20</sup>	
	435	434		409 <sup>19</sup>				
	445	448						
$\nu(\text{S-H})$	2520	2517		2525 <sup>23</sup>				

<sup>a</sup> Local  $T_d$  point group symmetry is assumed for isolated  $\text{GeS}_4^{4-}$  units. Assignments for comparable reference systems are also presented. All units are in wavenumbers ( $\text{cm}^{-1}$ ). <sup>b</sup> Although controversial, in glassy  $\text{GeS}_2$  the  $\text{A}_1$  companion band is often attributed to edge shared tetrahedral units.

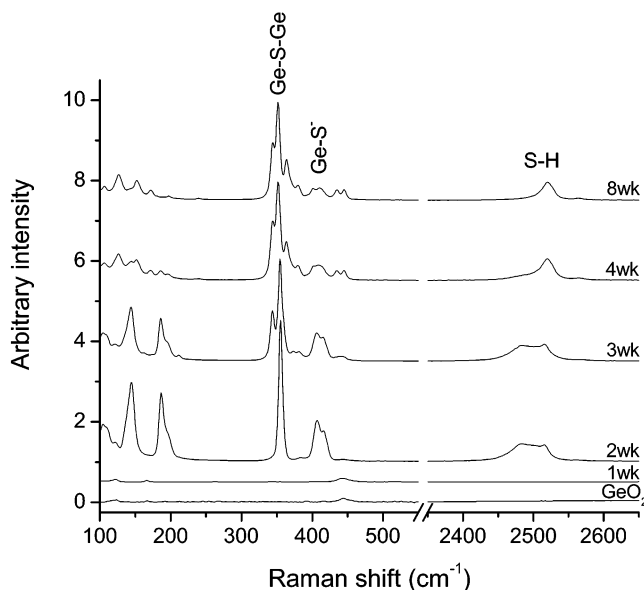


Figure 2. Raman spectra of  $\text{GeO}_2$  reacted with liquid  $\text{H}_2\text{S}$  at room temperature as a function of time. No reaction is noted for 1 week; 2-week reaction time produces a highly vibrational symmetric adamantane  $\text{H}_4\text{Ge}_4\text{S}_{10}$  phase; 3- and 4-week reaction times produce mixed phases, whereas 8 weeks of reaction time appears to produce an  $\text{H}_2\text{Ge}_4\text{S}_9$  phase with a more complex cage unit.

presents select Raman and IR vibrational mode assignments for the adamantane  $\text{H}_4\text{Ge}_4\text{S}_{10}$  phase and representative reference systems assuming  $T_d$  point group symmetry. In a polarized Raman spectrum, the strongest bands may be assigned to the  $3\text{A}_1$  vibrations for the adamantane structural unit.<sup>9</sup> In the

unpolarized spectrum obtained for 2 weeks of reaction time, the strongest intensity band observed at  $\sim 355 \text{ cm}^{-1}$  is assigned to  $\text{Ge-S-Ge}$  symmetrical bridge-stretching mode  $\nu_2(\text{A}_1)$ . This value is within resolution for that reported for  $\text{Na}_4\text{Ge}_4\text{S}_{10}$ .<sup>3</sup> The band observed at  $\sim 187 \text{ cm}^{-1}$  may be assigned to  $\text{Ge-S-Ge}$  symmetrical bridge bending mode  $\nu_3(\text{A}_1)$ . The two overlapping bands centered around  $\sim 407$  and  $\sim 416 \text{ cm}^{-1}$  may be attributed to  $\text{Ge-S}^-$  nonbridging or symmetrical terminal stretching mode  $\nu_1(\text{A}_1)$ . This is consistent with two broad bands with peak intensities located around  $\sim 2484$  and  $\sim 2515 \text{ cm}^{-1}$  assigned to  $\text{S-H}$  bond stretching. Two distinct bands indicate two unique hydrogen environments for the  $\text{H}_4\text{Ge}_4\text{S}_{10}$  phase.

The products associated with 3 and 4 weeks of reaction time suggest mixed phases, whereas the product from 8 weeks of reaction time indicates a different structure all together. Although it is not possible to fully resolve this new structure from the unpolarized Raman spectrum alone, inferences may be drawn from comparisons with established systems. Without knowing the structure, one may consider the individual  $\text{GeS}_4^{4-}$  units possessing  $T_d$  symmetry to suggest mode assignments using crystalline and glassy  $\text{GeS}_2$  as references. Table 2 presents Raman and IR suggested vibrational mode assignments of the  $\text{H}_2\text{Ge}_4\text{S}_9$  phase for 8 weeks of reaction time. In the spectrum, medium-intensity vibrational bands at  $\sim 106$ ,  $\sim 127$ ,  $\sim 152$ , and  $\sim 172 \text{ cm}^{-1}$  and weak-intensity bands at  $\sim 197$  and  $\sim 240 \text{ cm}^{-1}$  are located in the frequency region consistent with translational, rotational, and bond-bending E and lower frequency  $\text{F}_2$  modes.<sup>14-16</sup> The strongest bands with peak intensity values at  $\sim 344$ ,  $\sim 352$ , and  $\sim 363 \text{ cm}^{-1}$  may be attributed to  $\text{Ge-S-Ge}$  stretching modes. Specifically, the bands at  $\sim 344$  and  $\sim 352 \text{ cm}^{-1}$  may be attributed to  $\text{A}_1$  symmetric stretching due to weak



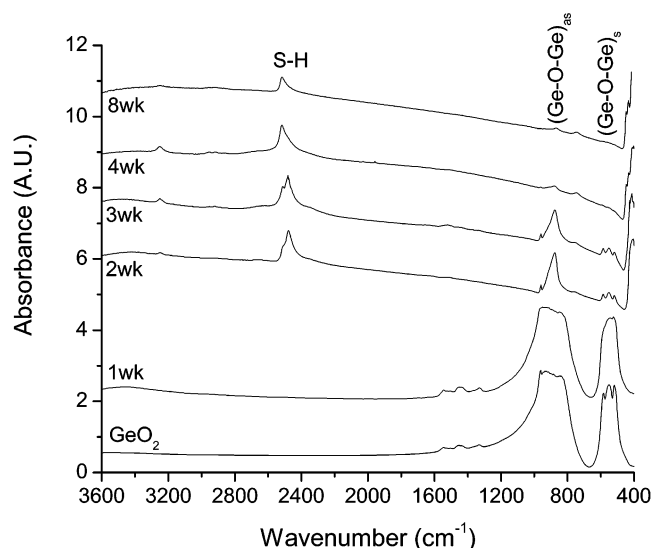


**Figure 3.** Mid-IR spectra of  $\text{GeO}_2$  reacted with liquid  $\text{H}_2\text{S}$  at room temperature as a function of time. No reaction is noted for 1 week; 2-week reaction time produces an S–H stretching mode around  $2500\text{ cm}^{-1}$  that becomes less IR active with increased reaction time. Vibrational modes associated with the starting  $\text{GeO}_2$  reduce in intensity with increasing reaction time.

IR activity. In contrast, the band at  $\sim 363\text{ cm}^{-1}$  may be attributed to  $F_2$  asymmetric stretching due to strong IR activity. The ratio of the band intensities at  $\sim 344$  and  $\sim 352\text{ cm}^{-1}$  are roughly consistent with corner-shared and edge-shared tetrahedral units, respectively, associated within the double-decker isomer. Note, the  $\sim 344\text{ cm}^{-1}$  band intensity was observed to increase after the mass of the reaction product stabilized, implying bridging of discrete units into rings and/or chains. The medium-intensity vibrational bands with peak intensities located at  $\sim 380$ ,  $\sim 401$ ,  $\sim 409$ ,  $\sim 435$ , and  $\sim 445\text{ cm}^{-1}$  may be generally attributed to  $A_1$  terminal stretching mode and higher  $F_2$  stretching modes.<sup>15</sup> Specifically, the broad band located at  $\sim 409\text{ cm}^{-1}$  is close to the  $\text{Ge-S}^-$  nonbridging mode for the 2-week reaction time. The S–H bond stretching mode for the 8-week reaction time has a strong intensity peak located  $\sim 2520\text{ cm}^{-1}$ ; this peak is narrower in frequency and half the integrated area of the S–H stretching mode for the 2-week reaction. This indicates one unique hydrogen environment for the  $\text{H}_2\text{Ge}_4\text{S}_9$  phase.

The Raman spectrum resulting from 8 weeks of reaction time is more consistent with an isomer having reduced vibrational symmetry and a more complex cage unit. Again, it is suggested that intact  $\text{Ge}_4\text{S}_{10}^{4-}$  unit cages are linked together to form rings and/or chains. The possible formation of a double-decker isomer of  $\text{Ge}_4\text{S}_{10}^{4-}$  units may be the result of extensive reaction time with hydrostatic pressure equal to that of the vapor pressure of  $\text{H}_2\text{S}$  at room temperature, i.e., 267 psia (1.8 MPa).

**3.3 Infrared Spectra.** Figure 3 presents the mid-IR spectra of the stabilized products as a function of reaction time in liquid  $\text{H}_2\text{S}$  at room temperature. For 1 week of reaction time, the resulting spectrum looks very similar to that of the starting  $\text{GeO}_2$  compound. The broad bands located around  $\sim 877$  and  $\sim 553\text{ cm}^{-1}$  may be assigned to  $\text{Ge-O-Ge}$  asymmetric stretching modes  $\nu_{\text{as}}$  ( $860, 894, 989\text{ cm}^{-1}$ ) and  $\text{Ge-O-Ge}$  symmetric stretching modes  $\nu_{\text{s}}$  ( $464, 569\text{ cm}^{-1}$ ), respectively.<sup>17</sup> Additionally, a weak O–H stretching mode centered around  $\sim 3400\text{ cm}^{-1}$  is present and is consistent with the hydration process as the first step of the total reaction. For a reaction time of 2 weeks, the corresponding mid-IR spectrum shows a reduction in the intensity of  $\text{Ge-O-Ge}$  asymmetric stretching and symmetric stretching modes. Two overlapping S–H stretching modes

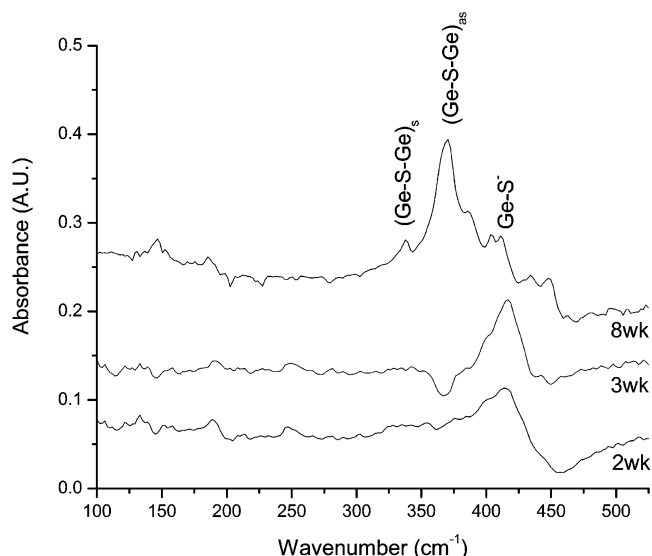
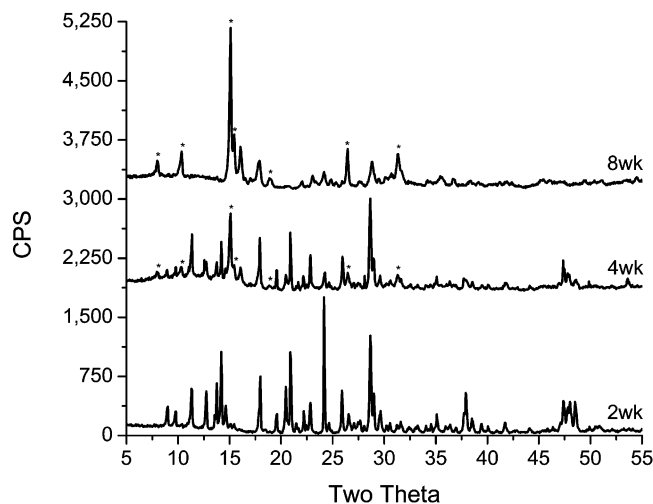


**Figure 4.** Far-IR spectra of  $\text{GeO}_2$  reacted with liquid  $\text{H}_2\text{S}$  at room temperature as a function of time. Two and three-week reaction times produce IR active  $\text{Ge-S}^-$  terminal stretching modes at  $\sim 414\text{ cm}^{-1}$ . Eight-week reaction time produces additional IR active modes including the strong asymmetric stretching mode at  $\sim 370\text{ cm}^{-1}$ .

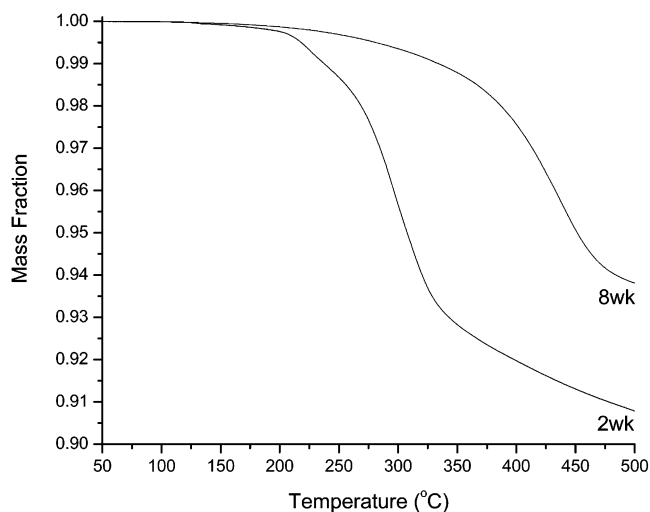
centered around  $\sim 2479$  and  $\sim 2511\text{ cm}^{-1}$  are also present. As noted from the corresponding Raman spectrum, the presence of two distinct bands indicates two unique hydrogen environments. For reaction times longer than 4 weeks, the  $\text{Ge-O-Ge}$  modes are almost completely absent. Additionally, the S–H stretching mode becomes less IR active, narrower in width, and located at a higher frequency with a peak intensity around  $\sim 2517\text{ cm}^{-1}$ . As with the corresponding Raman spectrum, this suggests only one unique hydrogen environment is present.

Figure 4 presents the far-IR spectra of stabilized products as a function of reaction time in liquid  $\text{H}_2\text{S}$  at room temperature. The products from 2 and 3 weeks of reaction time are less IR active compared with that from 8 weeks of reaction time. On the basis of the corresponding Raman spectrum, an adamantane structure having a point symmetry group of  $T_d$  is suggested for the 2-week reaction-time product. The band center at  $\sim 414\text{ cm}^{-1}$  may be partially attributed to the  $\text{Ge-S}^-$  terminal stretching mode  $\nu_1(A_1)$ . Infrared activity of this mode indicates a reduction in local  $T_d$  symmetry to at least  $C_{3v}$  symmetry with a terminal bond to hydrogen.<sup>18</sup> Additional asymmetric modes may also contribute to the broad feature in this frequency range, specifically  $\nu_{11}(F_2)$  and  $\nu_{10}(F_2)$  were reported at  $395$  and  $455\text{ cm}^{-1}$ , respectively, for  $\text{Cs}_4\text{Ge}_4\text{S}_{10}$ .<sup>9</sup> Bands were also observed for  $\text{Na}_4\text{Ge}_4\text{S}_{10}$  at  $390, 405, 420, 440,$  and  $455\text{ cm}^{-1}$ .<sup>7</sup>

The far-IR spectrum of the 3-week reaction-time product contains the same gross features as the 2-week reaction-time product. The far-IR spectrum of the compound produced with 8 weeks of reaction time is notably different. As with the corresponding Raman spectrum interpretation, individual  $\text{GeS}_4^{4-}$  units possessing  $T_d$  symmetry may be considered. The dominant band with a peak intensity located at  $\sim 370\text{ cm}^{-1}$  may be assigned to the  $F_2$  asymmetric bridge stretching mode; the  $\sim 7\text{ cm}^{-1}$  shift in frequency from that observed in Raman,  $\sim 363\text{ cm}^{-1}$ , may be the result of intermolecular coupling of tetrahedral units through bridging sulfur atoms.<sup>19</sup> The weak peak observed at  $\sim 338\text{ cm}^{-1}$  may be attributed to the  $A_1$  symmetric bridge stretching mode. IR activity of this peak infers that perfect  $T_d$  point group symmetry is not present.<sup>20</sup> Vibrational bands located at  $\sim 386, \sim 403, \sim 411, \sim 434,$  and  $\sim 448\text{ cm}^{-1}$  are in close agreement with those observed in the Raman spectrum. The



**Figure 5.** XRD spectra of  $\text{GeO}_2$  reacted with liquid  $\text{H}_2\text{S}$  at room temperature as a function of time. Unique crystalline phases are realized for reaction times of 2 and 8 weeks; 4 weeks produces a mixed phase. Asterisks are drawn to aid the identification of the 8-week structure in the four 4-week mixed phase using distinguishable peaks.



**Figure 6.** TGA spectra of  $\text{GeO}_2$  reacted with liquid  $\text{H}_2\text{S}$  at room temperature as a function of time. A reaction time of 2 weeks produces a less thermally stable phase than that of 8 weeks. Theoretical decomposition from pure  $\text{H}_4\text{Ge}_4\text{S}_{10}$  and  $\text{H}_2\text{Ge}_4\text{S}_9$  thiogermanic acids to germanium disulfide is realized at 0.89 and 0.94 mass fractions, respectively.

location of these bands is again consistent with  $A_1$  terminal stretching and higher  $F_2$  stretching modes. The complex IR and Raman spectra suggest a more complex structural cage unit.

**3.4. X-ray Diffraction.** Figure 5 presents the raw powder XRD spectra of the stabilized products as a function of reaction time in liquid  $\text{H}_2\text{S}$  at room temperature. Peaks corresponding to the starting quartz-type  $\text{GeO}_2$  were not readily identified in the resulting spectra. Unique phases were evident for the 2- and 8-week reaction times; the 4-week reaction time produced a mixed phase. The diffractogram for the 2-week reaction time product possesses peaks located at  $8.97^\circ$  and  $9.76^\circ$   $2\theta$ , indicating crystal periodicity up to  $9.858 \text{ \AA}$  and  $9.062 \text{ \AA}$ , respectively. The diffractogram corresponding to 8 weeks of reaction time is notably simpler, suggesting a more symmetric unit cell. Low angle diffraction peaks are located at  $8.01^\circ$  and  $10.35^\circ$   $2\theta$ , indicating crystal periodicity up to  $11.038 \text{ \AA}$  and  $8.547 \text{ \AA}$ , respectively. The growth of single crystals and XRD structural solutions are not yet performed for the product from 8 weeks

of reaction time; thus the existence of a double-decker complex isomer remains unresolved.

**3.5. Thermal Analysis.** Figure 6 presents the TGA spectra of the stabilized products of 2- and 8-week reaction times in liquid  $\text{H}_2\text{S}$  at room temperature. Decomposition onset temperatures corresponding to the 2-week reaction product  $\text{H}_4\text{Ge}_4\text{S}_{10}$  and the 8-week reaction product  $\text{H}_2\text{Ge}_4\text{S}_9$  were observed at  $\sim 250^\circ\text{C}$  and  $\sim 360^\circ\text{C}$ , respectively. Theoretical decomposition of pure phases of  $\text{H}_4\text{Ge}_4\text{S}_{10}$  and  $\text{H}_2\text{Ge}_4\text{S}_9$  into  $\text{GeS}_2$  would produce final mass fractions of 0.89 and 0.94, respectively. Thermal relaxation of the 8-week reaction product converting to the adamantane structural unit before decomposition was not observed in the corresponding Raman spectra; initial decomposition of both phases formed a glassy  $\text{GeS}_2$  product. After decomposition at  $500^\circ\text{C}$ , the observed Raman spectra of both isomers exhibited a strong Ge–S–Ge symmetrical bridge stretching mode at  $\sim 360 \text{ cm}^{-1}$ ; upon further heating ( $\sim 700^\circ\text{C}$ ), this band grew in intensity producing Raman spectra which were consistent with that reported for the high temperature 2-D crystalline  $\text{GeS}_2$  (denoted as  $\beta\text{-GeS}_2$  in this article).<sup>15</sup>

## 4. Conclusions

Novel reactions of liquid  $\text{H}_2\text{S}$  with  $\text{GeO}_2$  produce  $\text{Ge}_4\text{S}_{10}^{4-}$  ions in solution. These reactions involve kinetic processes including hydroxide to hydrosulfide group transformation, adamantane cage formation, and cage restructuring. Evaporating the  $\text{H}_2\text{O-H}_2\text{S}$  solution leaves thermally unstable  $\text{H}_4\text{Ge}_4\text{S}_{10} \cdot x\text{H}_2\text{O}$  units that decompose into the thermally stable anhydrous  $\text{H}_4\text{Ge}_4\text{S}_{10}$  or  $\text{H}_2\text{Ge}_4\text{S}_9$  phases. In general, the adamantane  $\text{H}_4\text{Ge}_4\text{S}_{10}$  phase is obtained from shorter reaction times, whereas an  $\text{H}_2\text{Ge}_4\text{S}_9$  phase with a more complex cage unit and a more symmetric unit cell is suggested for longer reaction times. The Raman, IR, and XRD structural evolution as a function of reaction time indicates a strongly kinetically controlled formation rate with presumably the hydrostatic pressure of liquid  $\text{H}_2\text{S}$  as the driving force. Ultimately, this  $\text{H}_2\text{Ge}_4\text{S}_9$  phase realized from longer reaction times is approximately  $110^\circ\text{C}$  more thermally stable than that of the adamantane  $\text{H}_4\text{Ge}_4\text{S}_{10}$  phase. For both thiogermanic acids, however, the thermal decomposition product is determined to be glassy  $\text{GeS}_2$  from corresponding Raman spectra.

**Acknowledgment.** This material is based on the work funded by the United States Department of Energy's Hydrogen Program under Cooperative Agreement No. DE-FC36-00GO1-531. Chad Martindale is thanked for help in obtaining far-IR spectra.

## References and Notes

- (1) Willard, H. H.; Zuehlke, C. W. The preparation and properties of potassium thiogermanate and thiogermanic acid; *J. Am. Chem. Soc.* **1943**, *65*, 1887–1889.
- (2) Poling, S. A.; Nelson, C. R.; Sutherland, J. T.; Martin, S. W., to be submitted.
- (3) Barrau, B.; Ribes, M.; Maurin, M.; Kone, A.; Souquet, J. L. Glass formation, structure and ionic conduction in the  $\text{Na}_2\text{S-GeS}_2$  system; *J. Non-Cryst. Solids* **1980**, *37*, 1–14.
- (4) Klepp, K. O.; Fabian, F. New chalcogenogermanates with adamantane type complex anions: preparation and crystal structures of  $\text{K}_4\text{Ge}_4\text{S}_{10}$ ;  $\text{Rb}_4\text{Ge}_4\text{S}_{10}$ ;  $\text{Rb}_4\text{Ge}_4\text{Se}_{10}$ , and  $\text{Cs}_4\text{Ge}_4\text{Se}_{10}$ ; *Z. Naturforsch., B: Chem. Sci.* **1999**, *54*, 1499–1504.
- (5) Klepp, K. O.; Zeitlinger, M. Crystal structure of tetracesium decasulfidotetragermanate,  $\text{Cs}_4\text{Ge}_4\text{S}_{10}$ ; *Z. Kristallogr.* **2000**, *215*, 7–8.
- (6) Eulenberger, V. G. Die Kristallstruktur des Thallium(I)thiogermanats  $\text{Tl}_4\text{Ge}_4\text{S}_{10}$ ; *Acta Crystallogr.* **1976**, *B32*, 3059–3063.

- (7) Ribes, M.; Olivier-Fourcade, J.; Philippot, E.; Maurin, M. Structural study of thio compounds with tetrane type anionic groups. Sodium thiosilicate ( $\text{Na}_4\text{Si}_4\text{S}_{10}$ ), sodium thiogermanate ( $\text{Na}_4\text{Ge}_4\text{S}_{10}$ ), and barium thiogermanate ( $\text{Ba}_2\text{Ge}_4\text{S}_{10}$ ); *J. Solid State Chem.* **1973**, *8*, 195–205.
- (8) Pohl, V. S.; Krebs, B. Darstellung und Struktur von  $\text{Cs}_4\text{Ge}_4\text{S}_{10} \cdot 3\text{H}_2\text{O}$ ; *Z. Anorg. Chem.* **1976**, *424*, 265–272.
- (9) Muller, A.; Cyvin, B. N.; Cyvin, S. J.; Pohl, S.; Krebs, B. Spectroscopic studies of  $\text{As}_4\text{O}_6$ ,  $\text{Sb}_4\text{O}_6$ ,  $\text{P}_4\text{S}_{10}^{4-}$  and organometallic compounds containing the  $M_4X_6$  cage. The Raman and IR spectrum of  $\text{Ge}_4\text{S}_{10}^{4-}$ ; *Spectrochim. Acta* **1976**, *32A*, 67–74.
- (10) Philippot, E.; Ribes, M.; Lindqvist, O. Crystal structure of sodium germanium sulfide ( $\text{Na}_4\text{Ge}_4\text{S}_{10}$ ); *Rev. Chim. Miner.* **1971**, *8*, 477–489.
- (11) Ando, W.; Kadowaki, T.; Kabe, Y.; Ishii, M. A Germanium Sesquisulfide,  $(t\text{BuGe})_4\text{S}_6$ , without Adamantane Structure; *Angew. Chem., Int. Ed. Engl.* **1992**, *31*, 59–61.
- (12) Unno, M.; Kawai, Y.; Shioyama, H.; Matsumoto, H. Synthesis, Structures, and Properties of Tricyclotetrasilachalcogenanes ( $\text{Thex}_2\text{Si}_2\text{E}_2$ )- $\text{E}_2$  (E = S, Se) and Tricyclotetragermachalcogenanes ( $\text{Thex}_2\text{Ge}_2\text{E}_2$ )- $\text{E}_2$  (E = S, Se); *Organometallics* **1997**, *16*, 4428–4434.
- (13) Mernagh, T. P.; Liu, L.-g. Temperature dependence of Raman spectra of the quartz- and rutile-types of  $\text{GeO}_2$ ; *Phys. Chem. Miner.* **1997**, *24*, 7–16.
- (14) Kotsalas, I. P.; Raptis, C. High-temperature structural phase transitions of  $\text{Ge}_x\text{S}_{1-x}$  alloys studied by Raman spectroscopy; *Phys. Rev. B* **2001**, *64*, 125210-1–125210-8.
- (15) Inoue, K.; Matsuda, O.; Murase, K. Raman spectra of tetrahedral vibrations in crystalline germanium dichalcogenides,  $\text{GeS}_2$  and  $\text{GeSe}_2$ , in high and low temperature forms; *Solid State Commun.* **1991**, *79*, 905–910.
- (16) Julien, C.; Barnier, S.; Massot, M.; Chbani, N.; Cai, X.; Loireau-Lozac'h, A. M.; Guittard, M. Raman and infrared spectroscopic studies of Ge–Ga–Ag sulphide glasses; *Mater. Sci. Eng.* **1994**, *B22*, 191–200.
- (17) Efimov, A. M. Infrared spectra, band frequencies and structure of sodium germanate glasses; *Phys. Chem. Glasses* **1999**, *40*, 199–206.
- (18) Kamitsos, E. I.; Kapoutsis, J. A.; Chryssikos, G. D.; Taillades, G.; Pradel, A.; Ribes, M. Structure and optical conductivity of silver thiogermanate glasses; *J. Solid State Chem.* **1994**, *112*, 255–261.
- (19) Lucovsky, G.; deNeufville, J. P.; Galeener, F. L. Study of the optic modes of  $\text{Ge}_{0.30}\text{S}_{0.70}$  glass by infrared and Raman spectroscopy; *Phys. Rev. B* **1974**, *9*, 1591–1597.
- (20) Kawamoto, Y.; Kawashima, C. Infrared and Raman spectroscopic studies on short-range structure of vitreous  $\text{GeS}_2$ ; *Mater. Res. Bull.* **1982**, *17*, 1511–1516.
- (21) Souquet, J. L.; Robinel, E.; Barrau, B.; Ribes, M. Glass formation and ionic conduction in the  $\text{M}_2\text{S}-\text{GeS}_2$  (M = Li, Na, Ag) systems; *Solid State Ionics* **1981**, *3–4*, 317–321.
- (22) Popovic, Z. V.; Holtz, M.; Reimann, K.; Syassen, K. High-pressure Raman scattering and optical absorption study of  $\beta\text{-GeS}_2$ ; *Phys. Status Solidi B* **1996**, *198*, 533–537.
- (23) Liu, X.; Tikhomirov, V.; Jha, A. Influence of vapor-phase reaction on the reduction of  $\text{OH}^-$  and S–H absorption bands in  $\text{GeS}_2$ -based glasses for infrared optics; *J. Mater. Res.* **2000**, *15*, 2864–2874.